

---

# Preliminary Evaluation of a Fuzzy Logic–Based Automatic Quantitative Analysis in Myocardial SPECT

Florent Cachin, MD<sup>1</sup>; Janusz Lipiecki, MD<sup>2</sup>; Danièle Mestas, MD<sup>1</sup>; Aimé Amonchot, MD<sup>2</sup>; Benjamin Geissler, MD<sup>1</sup>; Cyril Thouly, PhD<sup>1</sup>; Jean Ponsonnaille, MD<sup>2</sup>; and Jean Maublant, MD, PhD<sup>1</sup>

<sup>1</sup>Division of Nuclear Medicine, Jean Perrin Cancer Center, Clermont-Ferrand, France; and <sup>2</sup>Department of Cardiology, Gabriel Montpied University Hospital, Clermont-Ferrand, France

---

This study validates a new quantitative myocardial perfusion SPECT software. **Methods:** The processing starts with the extraction of the morphologic skeleton of the left ventricular myocardium from reconstructed transverse sections. Fuzzy logic is used to decide whether a pixel belongs to the myocardium and any perfusion defect is filled according to a truncated bullet model. The resulting image is partitioned in 18 isovolumetric sectors. Sex-matched normal limits, criteria of abnormality for rest <sup>201</sup>Tl and <sup>99m</sup>Tc-labeled perfusion tracers, reproducibility studies, and detection of coronary artery disease were developed and validated in an overall population of 343 patients. The sex- and tracer-matched means and SDs of a normal response were calculated in 93 male and 93 female patients with a <5% likelihood of coronary artery disease. Reproducibility measurements and assignment of different sectors of the myocardium to a specific coronary were performed from data collected in 49 and 60 patients, respectively. The accuracy of the detection of a coronary artery occlusion was assessed in 48 patients who also underwent coronary angiography. **Results:** The intra- and interoperator reproducibility of the sectorial activity was high with a linear regression coefficient of 0.97 and a SD of the difference measurement at 4.4% and 3.8%, respectively. Overall sensitivity and specificity for the detection of occluded coronary artery were 90% and 80%, respectively. For the detection of left anterior descending, left circumflex, and right artery coronary occlusion, sensitivity was 92%, 75%, and 92.5%, respectively, and specificity was 75%, 78%, and 90%, respectively. **Conclusion:** The new quantitative myocardial perfusion SPECT software appears to be a very helpful program for the objective analysis of perfusion tracer distribution in myocardial SPECT and a very accurate tool in the detection and localization of coronary artery occlusion.

**Key Words:** myocardial perfusion imaging; quantification; reproducibility; coronary artery disease

**J Nucl Med 2003; 44:1625–1632**

**T**he interpretation of myocardial blood flow images has been greatly improved by the use of SPECT, but it has also led to the need for a more precise analysis of the distribution of activity in the left ventricular (LV) myocardium. Quantitative techniques have been developed, derived from the analysis of circumferential profiles such as bull's eye analysis (1,2), or based on a volumetric sectorization (3–7). Almost all approaches remain operator dependent, a crucial limitation for the comparison between paired stress and rest studies. Another limitation of some of these methods is a high false-positive rate in the detection of coronary artery disease, which limits their use in clinical practice. We have previously developed an automatic method for the reorientation of the LV long axis, a necessary preliminary step for a precise quantitative analysis (8,9). We now describe a new and original approach to quantitative perfusion SPECT involving principles of mathematic morphology and fuzzy logic and providing a fully automatic sectorization of the normal and abnormal LV. This study was designed to develop sex-specific normal limits to assess the reproducibility and the accuracy in detecting and localizing coronary artery disease with this new software.

## MATERIALS AND METHODS

### SPECT Acquisition and Processing

Thirty minutes after tracer injection, patients were placed in supine position. Using a single-head gamma camera (Sopha DSX; General Electric Medical Systems) equipped with a low-energy, high-resolution collimator, 32 projections of 40 s (<sup>201</sup>Tl) or 30 s (<sup>99m</sup>Tc) each were acquired over 180° as a 64 × 64 matrix (0.64-cm pixel size). For <sup>99m</sup>Tc-labeled tracers, a 20% window was centered over the 140-keV photopeak. For <sup>201</sup>Tl, a 20% window centered over the 69- to 83-keV energy domain and a 20% window centered over the 167-keV photopeak were selected. No scatter or attenuation correction was applied. The sections were reconstructed using a filtered backprojection algorithm with a Butterworth filter of order 5 and 0.25 pixel<sup>-1</sup> cutoff.

Transverse sections were automatically centered, reoriented, and zoomed (×2) using a commercial software from the same manufacturer (MyoSPECT; General Electric Medical Systems).

---

Received Feb. 12, 2003; revision accepted May 20, 2003.

For correspondence or reprints contact: Jean Maublant, MD, PhD, Jean Perrin Cancer Center, 58, rue Montalembert, Cedex 1, 63011 Clermont-Ferrand, France.

E-mail: jean.maublant@cjp.fr

The myocardial tracer distribution was quantified with the Myoflex program now available in the same software package.

As described earlier (10), the first step of Myoflex grossly isolates the normal myocardium within the area defined by the 50% of maximum activity threshold. Then, a 3-dimensional (3D) skeletonization process (11–13) is applied. The algorithm removes particular voxels called simple points (14), which are recognized through the value of 2 multiparametric variables or topologic numbers as defined in mathematic morphology. The result is a 3D surface centered in the LV myocardium. This skeleton is enriched by attributing to each of its pixels the value of its shortest discrete distance to the outer limits of the 50% threshold. Therefore, that structure corresponds to a compressed view of the LV myocardium.

In patients presenting with a defect, the interrupted skeleton is rendered continuous by interpolating between its borders and fitting the model of a “truncated bullet” adjusted from statistical data (15). After that geometric reconstruction (16) and to facilitate the segmentation of the myocardium, a new method based on a fuzzy logic approach has been developed (17). The original image was transformed into a functional image in which the value of each pixel contained its “degree of belonging” to the myocardium, a real value comprised in the [0,1] interval.

The degree of belonging was obvious for 2 sets of pixels: (a) those of the skeleton, because their degree of belonging to the myocardium is always 1; and (b) those of the edge of the frame, because their degree of belonging to the myocardium is always 0. All of the other pixels represented the fuzzy set. Their degree of belonging to the myocardium is comprised in the [0,1] interval. Its calculation was based on a fuzzy logic formula with 25 parameters (18) obtained by throwing from each pixel a series of beams in 8 directions until either a skeleton or an edge point was encountered. Each  $i$  beam extremity allowed definition of 3 parameters: (a) value of the skeleton—that is, Euclidean distance to the outer limit of the 50% thresholded myocardium, when the extremity was a skeleton pixel, 0 otherwise:  $f(i)$ ; (b) activity level of the extremity on the SPECT image:  $act(i)$ ; and (c) discrete length of the beam:  $d(i)$ . The last parameter was the activity on the SPECT image at the origin of the beam, called pixel  $p$ :  $act(p)$ . For each beam, the following  $\mu_i(p)$  parameter was calculated:

$$\mu_i(p) = \alpha \cdot d_{\max} \cdot \frac{act(p) - act(i)}{d(i) - f(i)}, \quad \text{Eq. 1}$$

in which  $\alpha$  is a normalization coefficient such as the sum of all  $\mu_i(p) = 1$ , and  $d_{\max}$  is the largest possible beam length. The degree of belonging of each pixel to the myocardium was finally obtained by adding the  $\mu_i(p)$  of the beams having their extremity in contact with the skeleton.

This algorithm was applied independently to sets of 2-dimensional horizontal and vertical long-axis sections. The final frames were a fusion of these 2 sets in which only the highest degree of belonging of each pixel was retained. The advantage of the generated functional image over the original activity image is that the myocardial area is represented with a much higher contrast (Fig. 1). The LV becomes, therefore, much easier to segment. A 20% threshold applied to this functional image converted it into a binary image that represents the whole LV, including the hypoactive or defect areas (Fig. 2). This process also stands for the delineation of the basal limits of the myocardium. The reconstructed LV is finally partitioned into 18 sectors of identical volume (Fig. 3). The mean

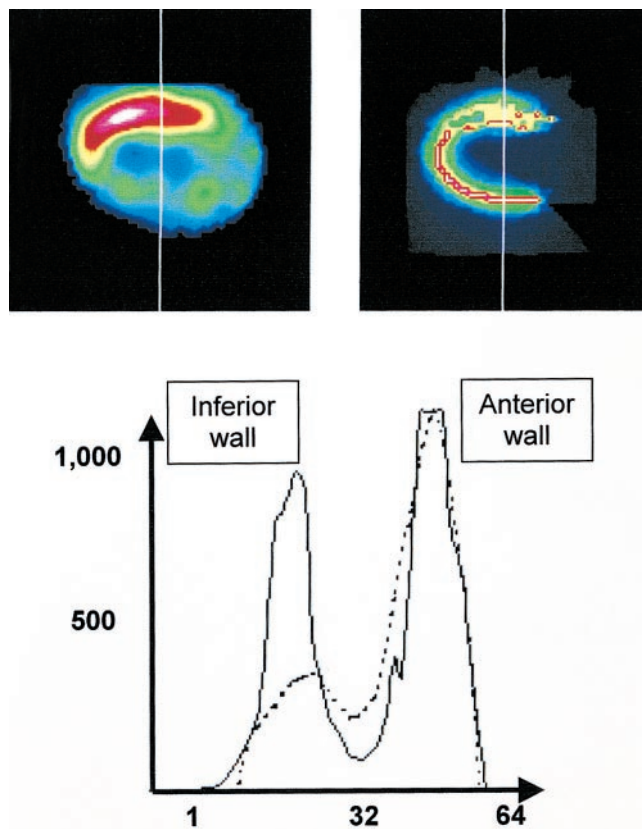


**FIGURE 1.** Activity profile (dashed line) and profile of corresponding degree of belonging (bold line) along vertical line in midportion of vertical long-axis section. Profiles were obtained from original SPECT image (left) and calculated image of degree of belonging (right), respectively. Large inferior defect seen on SPECT image disappears on functional image.

activity inside each sector is expressed in percentage relative to the activity of the sector with the highest value.

In practice, the operator is offered the possibility of correcting the automatic centering of the slices in 3D and modifying the proposed apical and basal limits of the LV mask. The reconstructed and completed 3D frame of the skeleton is displayed during the computation. The final screen (Fig. 4) shows the 4 central views of the short-axis, horizontal, and vertical long-axis sections, accompanied by a binary display of the corresponding reconstructed volumes (the reconstructed wall of the myocardium—that is, the part of the wall that corresponds to a hypoactive or defect area on the original image—is displayed in red; the normal wall is displayed in white). The 18 sectors are also displayed in 2 sets: one indicating the mean relative activity of each sector, and the other expressing that value in number of SDs by comparison with the normal database. These results are also color coded with a 3-level color scale (white for normal, yellow for hypoactive, red for defect). Because the program can process 2 sets of images (stress and rest), another part of the display shows the sector-by-sector difference between both studies.

#### Database of Normal Values

The mean and SD of the normal activity inside each sector were determined in a population of patients having a <5% likelihood of coronary artery disease based on the Bayesian analysis of age, sex,



**FIGURE 2.** Example of different steps of processing (left to right): original SPECT vertical long-axis section in patient with inferior infarction, binary thresholded image and its derived skeleton, completed skeleton, functional image of degree of belonging, and binary image completed with thresholded functional image.

and symptoms and on the results of their stress electrocardiogram (ECG). Three series of patients (Table 1) were studied supine at maximal stress (heart rate at tracer injection > 85% of maximal predicted heart rate) and at rest 4 h later: 58 patients (34 males, 24 females) with  $^{201}\text{Tl}$ , 88 patients (35 males, 53 females) with  $^{99\text{m}}\text{Tc}$ -sestamibi, and 40 patients (24 males, 16 females) with  $^{99\text{m}}\text{Tc}$ -tetrofosmin (this last series was kindly provided by Pierre Rigo, Liege, Belgium). The injected activity was 110 MBq at stress and 60 MBq at rest for  $^{201}\text{Tl}$  and 400 MBq at stress and 800 MBq at rest for the  $^{99\text{m}}\text{Tc}$  agents.

When a sector differed by >2 SD from its corresponding normal database mean value, it was considered as hypoactive. When it differed by >4 SD, it was considered as a defect.

### Application to Patients with Coronary Artery Occlusion

Because one of the applications of the quantification program is to determine the number of involved vessels in coronary artery disease, we are proposing to match each sector with the left anterior descending artery (LAD), left circumflex artery (LCx), or right coronary artery (RCA). For that purpose, 31, 22, and 7 patients with a history of single-vessel myocardial infarction in the territory of the LAD, RCA, or LCx, respectively, at coronary angiography underwent a rest myocardial SPECT (Table 1) and a quantification analysis. The delay between angiography and SPECT was always <8 d. For each vessel and each sector S, a frequency abnormality ( $\text{FA}_s$ ) was calculated as the proportion of patients with an abnormal sector S among all patients with that coronary artery occluded. This provided us with 3  $\text{FA}_s$  for each sector. The  $\text{FA}_s$  with the highest value and that was >10% higher than the second  $\text{FA}_s$  was considered as indicating the involved coronary artery for that sector. If there was no "significant" difference between the 3  $\text{FA}_s$ —that is, no  $\text{FA}_s$  was superior by >10%

to any of the 2 other  $\text{FA}_s$ —the sector was not assigned to a coronary artery and considered as "not attributed."

Reproducibility of the program was measured in a maximum of 49 patients (Table 1). All acquisitions were performed at rest, with  $^{201}\text{Tl}$  or  $^{99\text{m}}\text{Tc}$  for 26 and 23 patients, respectively. The processing was performed twice by a well-trained operator and once by a less-trained operator. The interobserver reproducibility compared the results of the less-trained operator with the first measurement of the well-trained operator.

The accuracy of Myoflex in the detection of coronary artery occlusion was assessed in 48 patients having a clinical history or ECG evidence, or both, of at least 1 prior myocardial infarction. These patients underwent rest  $^{99\text{m}}\text{Tc}$ -tetrofosmin myocardial SPECT and coronary angiography (Table 1). There were 63 infarct-related coronary occlusions (28 LAD, 27 RCA, and 8 LCx) and 81 either normal or not occluded coronary arteries (20 LAD, 21 RCA, and 40 LCx). The median time between scintigraphy and angiography was 30 d (range, 8–60 d).

### Statistical Analysis

Statistical analysis of the reproducibility was based on linear regression and a Bland–Altman plot (19). ANOVA was used for the statistical comparison of the sectorial activity between the 3 tracers, between the rest and stress studies, and between the subgroups of male and female patients.

For overall detection of coronary artery occlusion, sensitivity was defined as the proportion of territories with abnormal SPECT among the territories with angiographic evidence of coronary artery occlusion. Specificity was defined as the proportion of patients with normal SPECT among the patients with normal coronary angiography. Sensitivity for detection of disease in a given coronary artery was defined as the proportion of patients with a SPECT defect in the studied territory among the patients with occlusion in the given coronary artery.

Specificity for detection of disease in a given coronary artery was defined as the proportion of patients with normal SPECT in the studied territory among the patients with a normal coronary artery in the studied coronary bed.

## RESULTS

### Normal Database

Once the mean and SD of the distribution of the 3 tracers have been obtained for each of the 18 sectors, we performed several cross-comparisons between the different groups of normal patients—that is, between the stress and rest studies performed with the same tracer and in patients of the same sex.

With all tracers and in 95% of all patients, sector 9 showed the highest activity. For all sectors, there was no

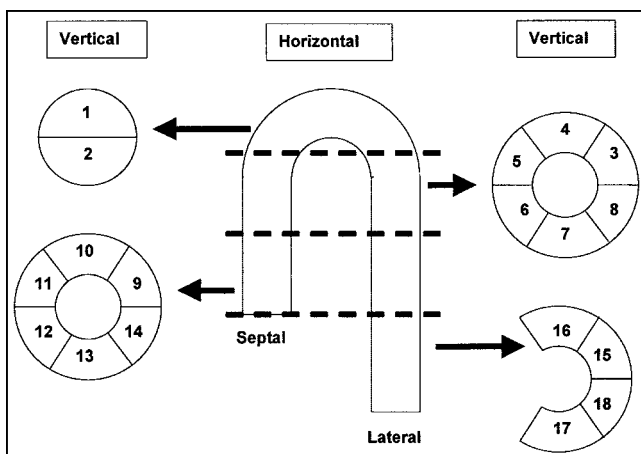


**FIGURE 3.** Organization of 18 sectors dividing LV wall in small elements of similar volume.

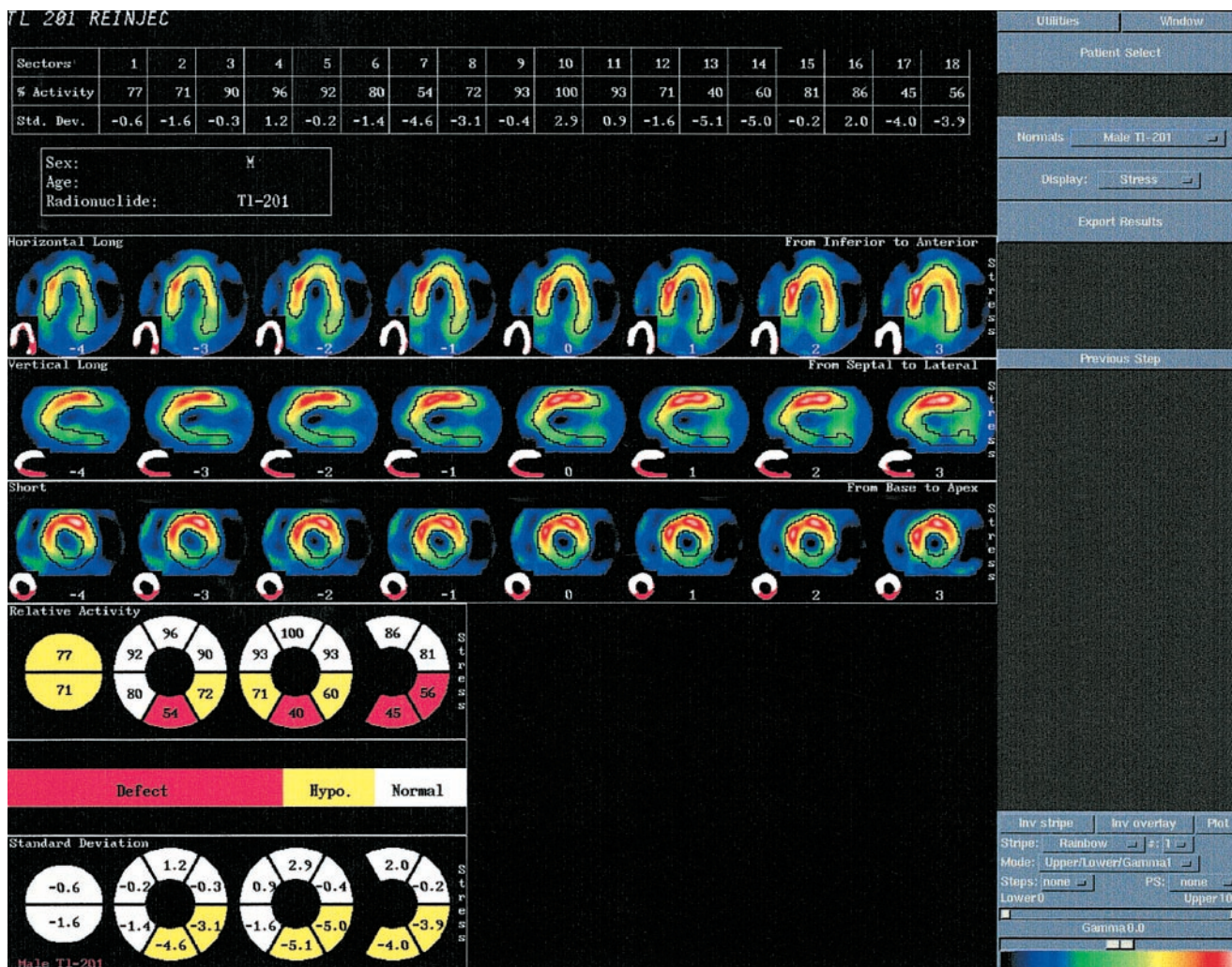


**FIGURE 4.** Final screen display of Myoflex program shows for each sector mean activity and SD (table in top, circles in bottom) and corrected slices (middle).

significant difference between stress and rest studies performed with the same tracer. That allowed us to pool these data. However, in at least 4 sectors, the activity was significantly different between male and female patients in studies performed with the same tracer. For that reason, Myoflex includes separate databases for male and female patients.

When  $^{99m}\text{Tc}$ -sestamibi,  $^{99m}\text{Tc}$ -tetrofosmin, and  $^{201}\text{Tl}$  were compared, there was no difference between  $^{99m}\text{Tc}$ -sestamibi

and  $^{99m}\text{Tc}$ -tetrofosmin. Therefore, we decided to pool these 2 databases in 1 single database. For  $^{201}\text{Tl}$ , quantification results per sector were statistically different from the pooled  $^{99m}\text{Tc}$  database, which explains why Myoflex includes a separate  $^{201}\text{Tl}$  database (Table 2).

In summary, these results justify that the Myoflex software contains 4 normal databases: male  $^{201}\text{Tl}$ , female  $^{201}\text{Tl}$ , male  $^{99m}\text{Tc}$ , and female  $^{99m}\text{Tc}$ . Each database contains the mean and SD for the 18 sectors.

**TABLE 1**  
Patient Characteristics of 4 Groups Included in Study

Study objectives	No. of patients	Acquisition conditions	Coronary artery disease
Normal database	186	Stress, rest: $^{201}\text{Tl}$ , $^{99m}\text{Tc}$	Low probability
Sector assignment	60	Rest: $^{99m}\text{Tc}$ , $^{201}\text{Tl}$	Single-vessel occlusion with myocardial infarct
Reproducibility	49	Stress, rest: $^{99m}\text{Tc}$ , $^{201}\text{Tl}$	High probability
Software performance	48	Rest: $^{99m}\text{Tc}$	From single- to triple-vessel disease with myocardial infarct

**TABLE 2**  
Comparison of Quantification Results Obtained with <sup>201</sup>Tl and <sup>99m</sup>Tc Agents

Comparison	Database		
	<sup>201</sup> Tl	<sup>99m</sup> Tc-Sestamibi	<sup>99m</sup> Tc-Tetrofosmin
Stress vs. rest	NS	NS	NS
Male vs. female*	$P < 0.05$	$P < 0.05$	$P < 0.05$
Male: <sup>201</sup> Tl database†	—	$P < 0.05$	$P < 0.05$
Female: <sup>201</sup> Tl database†	—	$P < 0.05$	$P < 0.05$
Male: <sup>99m</sup> Tc-sestamibi database†	$P < 0.05$	—	NS
Female: <sup>99m</sup> Tc-sestamibi database†	$P < 0.05$	—	NS
Male: <sup>99m</sup> Tc-tetrofosmin database†	$P < 0.05$	NS	—
Female: <sup>99m</sup> Tc-tetrofosmin database†	$P < 0.05$	NS	—

\*Stress and rest acquisition are pooled.

†Compared with SPECT performed with other tracers in group of same-sex patients.

NS = nonsignificant.

### Application to Patients with Coronary Artery Disease

In the attempt to assign each of the 18 sectors to a specific coronary artery, the FA<sub>s</sub> defined for each of the 3 arteries have been calculated. The analysis of these values yielded a predominant LAD in 8 sectors and LCx and RCA in 4 sectors each (Fig. 5). Two sectors could not be related to any predominant coronary artery bed.

The interoperator reproducibility of the sectorial activity was measured in 45 patients (882 sectors). Among those, intraoperator reproducibility was measured in 23 patients. The coefficient of correlation between 2 measurements performed by the same operator was 0.97. The Bland–Altman test (Fig. 6) showed a good reproducibility with a SD of difference and a mean difference of 4.3% and 0.5%, respectively. The interoperator (Fig. 7) SD of the difference and the mean difference were 3.8% and 0.15%, respectively, and the coefficient of correlation was 0.97.

In the 48 patients with prior myocardial infarction, the sensitivity and specificity of Myoflex for overall detection of coronary artery occlusion were 90% and 80%, respectively. The sensitivity for detection of disease in LAD, LCx, and RCA was 92%, 75%, and 92%, respectively. The specificity of vessel localization was 75%, 78%, and 90% for the LAD, LCx, and RCA, respectively (Fig. 8).

### DISCUSSION

Myoflex is aimed at the automatic sectorial quantification of a myocardial SPECT image, assuming that this image has

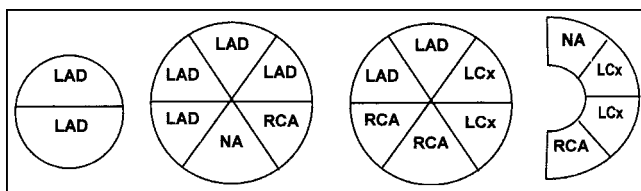


**FIGURE 5.** Correspondence between sectors and coronary artery. NA = not attributed.

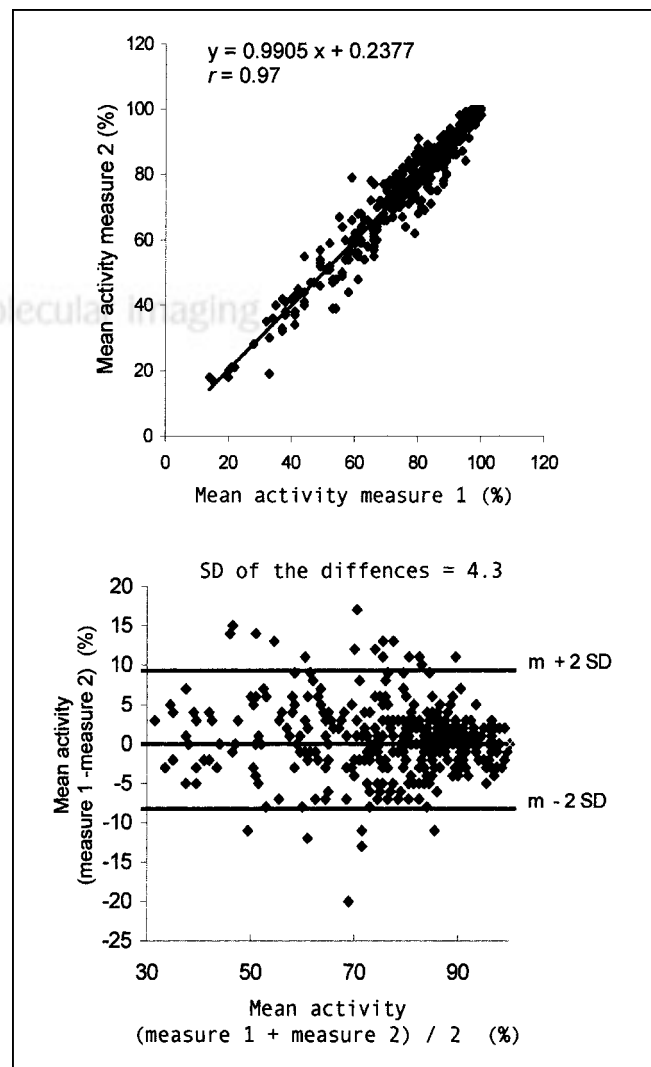


**FIGURE 6.** Intraobserver reproducibility of mean activity determined from 414 sectors of 23 patients with known coronary artery disease (top, linear regression analysis; bottom, Bland–Altman plot).

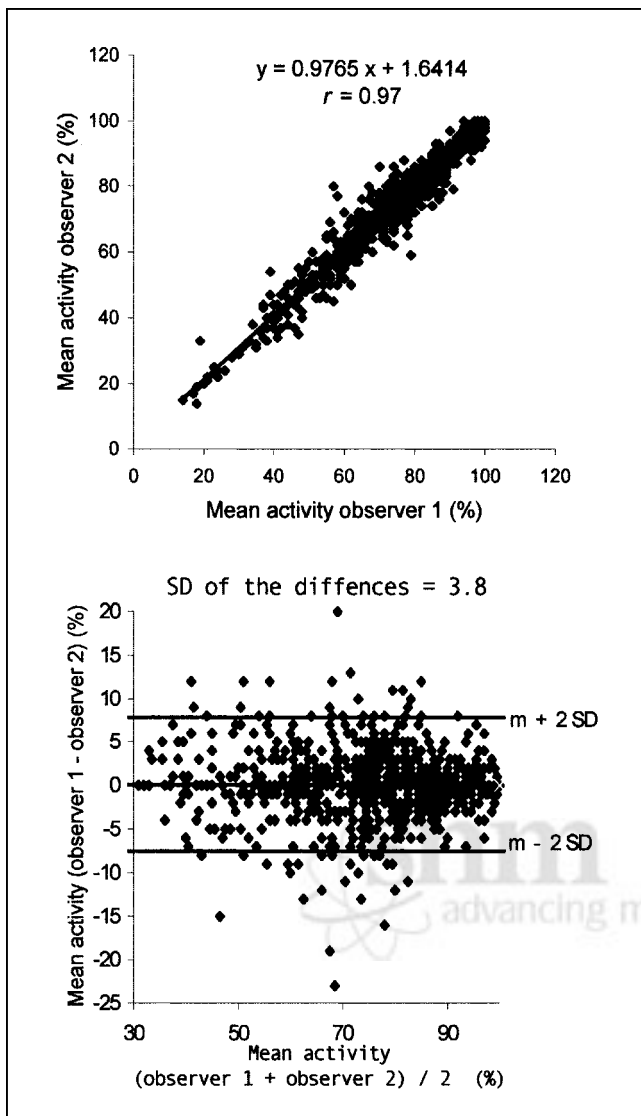


**FIGURE 7.** Interobserver reproducibility of mean activity determined from 882 sectors of 49 patients with known coronary artery disease (top, linear regression analysis; bottom, Bland-Altman plot).

been reoriented, zoomed, and isolated from extracardiac areas of high activity. The combination of mathematic morphology and fuzzy logic with classical fitting methods provides an overall analysis of the LV because the hypoactive and the normal areas are involved in the final presentation. This new approach should not be aggregated with neural nets or expert systems, which rest on fundamentally different methods. Even if the term “fuzzy logic” is used, it only refers to the fact that an image can be partitioned in a different way than through a direct binary approach—namely, the value of each pixel is modulated according to the value of the surrounding structures. But no learning process is integrated in the program. When applied to a study with the same parameters, the same results are always produced.

The high reproducibility of Myoflex is an encouraging step toward the automatic analysis of paired stress–rest studies. The robustness of the algorithm is possibly related to the combined application of mathematic morphology and fuzzy logic to scintigraphic imaging. The concept of skeleton was originally developed to describe the global properties of complex objects in a compact, highly structured way. To our knowledge, this is the first application of skeletonization to scintigraphic images (20).

In myocardial scintigraphy, segmentation is usually performed using threshold or edge detection techniques that allow extraction of normally perfused regions (21–23), but it cannot detect hypoperfused myocardial areas with a transmural defect. In his quantitative perfusion SPECT (QPS) software (3), Germano et al. define a quantification profile as pathologic if its peak count profile falls below 50% of the maximal myocardial count. In Myoflex, the fuzzy logic approach was chosen to overcome the limitation of using only a single parameter. Indeed, fuzzy logic is a multivariate logic that authorizes intermediate values to be defined, usually ranging continuously between 0 and 1 instead of using only 0 or 1. It was introduced by Zadeh (24) in 1965 as an attempt to apply a more human-like way of thinking in the programming of computers and to use parameters with intermediate levels instead of the binary levels such as yes/no, true/false, black/white, and so forth. Its principles started to be applied only recently to image processing, in particular, for segmentation. The fuzzy logic process can only be applied to a connected skeleton. In effect, the degree of belonging to the myocardium is computed by measuring discrete distances along beams that can intercept with the skeleton. A defect in the skeleton is responsible for an overestimated distance along the beams that could run across. Filling the disconnection, the so-called skeleton

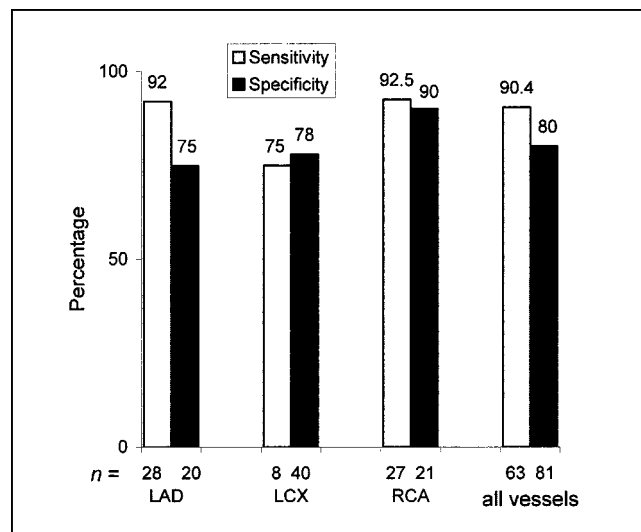


**FIGURE 8.** Sensitivity and specificity of myocardium rest SPECT quantification images for identification of disease in individual coronary arteries.

patching process, was achieved through modeling. The truncated bullet is a simple geometric model that generally fits well with the shape of the LV. The oblique surface of the basal part has been defined from the statistical analysis of the base of the myocardium in SPECT studies performed in patients with a low likelihood of coronary artery disease. Nevertheless, it sometimes happens that the limits chosen by the program do not fit with the particular shape of a given myocardium. It is also possible that a basal infarction seems to disorganize the structure of the LV base. For these reasons, the operator is offered the possibility of correcting manually the proposed basal limits of the LV myocardium. This maneuver irremediably alters the reproducibility of the technique, but at the advantage of more reliable results.

Even with the above limitations, reproducibility in the quantification of the 18 sectors appears excellent. The SEM and of the difference mean in Bland–Altman analysis is always <5% and the correlation coefficient is in the range of 0.97. The reproducibility study of QPS published by Germano et al. (3) has been performed with a semiquantitative scale of abnormality perfusion (0–4). Their results are excellent—in particular, the reproducibility ( $r = 0.99$ )—but the conversion of continuous to discrete values tends to maximize the agreement. On the other hand, the completely automated PERFIT software developed and described by Slomka et al. (6) results in the absence of any intraobserver variability (25), a result that can also be attained with Myoflex if the operator never corrects for the centering or the positioning of the basal limits. Finally, the method described by Benoit et al. (7), which is based on the quantification of activity profiles performed on radial slices, yields a reproducibility close of our method with a 2.4% SD. Because all of these methods were not available in our laboratory at the time of this study, we could not perform any comparison with Myoflex.

One of the goals of this study was to assess the capability of Myoflex in the identification of the individual vessels responsible for the ischemic disease. Like most of the other authors, we have calculated the frequency of an abnormal tracer distribution for each sector and for each coronary artery. In CEQUAL and in a former version of the Cedars Sinai software (1,26), a sector is matched to a specific coronary artery if this sector is abnormal in >80% of the patients with single-vessel disease in that artery. In the new version of the Cedars Sinai software, the method of calculation is announced to be different but this is not explained by its authors. Like these other methods, our algorithm results in a significant overlap at the boundaries of the 3 main coronary territories. Among the 18 sectors, only 2 sectors were not attributed to a specific coronary artery. These are the seventh and fifteenth sectors, which are uniformly associated with LAD, LCx, and RCA. To minimize this phenomenon, we have compared statistically the pathologic frequency per sector computed for each coronary. But, because of the small number of patients with a LCx artery occlusion, this method is not yet fully relevant.

A critical issue in the automatic analysis of myocardial SPECT images is the choice of a cutoff level between the normal and abnormal myocardium. Most authors use a receiver-operating-characteristic curve approach to establish the best cutoff value of defect size and the extent between stress and rest SPECT. This cutoff is expressed in percentage of the number of pathologic pixels among all pixels included in the coronary-related sector. This approach is not relevant in our method. The fuzzy logic algorithm is based on several parameters to decide if a pixel belongs to the myocardium and intrinsically assumed segmentation in 18 adjacent isovolumetric objects. Therefore, the minimal significant abnormality defect must involve at least 1 sector—namely, 5.5% of the myocardial volume.

None of the reported validation studies in quantitative myocardial SPECT has been based on a population with a prior myocardial infarction for testing its accuracy in detection and localization of a coronary artery occlusion. Indeed, the usual strategy is to validate the quantitative software in comparing stress and rest acquisitions to detect a stenosis of >50%–70%. For instance, methods using spheric or spherocylindrical sampling techniques generating maximal-count circumferential profiles have been reported to yield a high sensitivity for detection of coronary artery disease but also a low specificity, in the range of 50% (2,27). The QPS and PERFIT programs seem to result in a higher specificity in the range of 80%–90%. Our opinion is that using only stress–rest studies is not an optimal strategy to validate myocardial perfusion analysis software. Indeed, the first step should be to match as precisely as possible the territory of the diseased coronary artery with the myocardial sectors on SPECT. Utilizing a stress–rest protocol can only unveil a hemodynamically significant stenosis, but it is known that the degree of stenosis is difficult to appreciate on coronary angiography and that the functional consequence of a stenosis on the downstream tissue perfusion is highly variable, as demonstrated by intracoronary Doppler measurements (28,29). Therefore, the diseased coronary artery is not always responsible for a clear-cut defect on SPECT. These drawbacks disappear when patients with a prior myocardial infarction are studied at rest because the vessel is either occluded or patent. After this preliminary topographic validation step, the standard diagnosis performance evaluation will be performed.

Our quantification algorithm shows a high sensitivity (90%), which should provide its users with an easy detection and localization of coronary artery occlusion. Its specificity for RCA is in the same range. However, the specificity is lower (75%–78%) for LAD and LCx, which can be explained by the large defect size of the LAD infarcts, by the frequent overlapping between the territory of these 2 arteries as seen in sector 16, and by a hypothetical <85% stenosis with a hemodynamic consequence at rest. Besides these limitations, cumulating its sensitivity and specificity, Myoflex appears to be highly accurate in the detection and localization of coronary artery occlusion.

However, the utilization of Myoflex software is limited by a few factors. A learning phase in its use is mandatory, especially in the positioning of the LV center. Another critical step is also to correctly define the myocardial mask in the case of an apical defect. Indeed, a small mask could exclude the apex from the reconstruction process. In several places, data acquisition is performed with the patients in the prone position. It is very likely that the mean sectorial values obtained in individuals with a normal heart will be somehow different between prone and supine acquisition conditions. There might therefore be a need for the development of a set of normal database values in the prone position.

The next step in the validation of Myoflex will be to test its capability in detection of stress-induced ischemia with comparison between stress and rest data. We have already started to extend the skeleton concept to gated SPECT acquisitions for the measurement of ejection fraction, wall thickening, and wall motion quantification. This skeleton and fuzzy logic algorithm seems to remain fairly robust in these conditions (30), but further clinical validations are needed.

## CONCLUSION

Myoflex is a new myocardial quantitative SPECT software that is based on an original fuzzy logic approach. A normal database has been established for  $^{201}\text{Tl}$  and  $^{99\text{m}}\text{Tc}$  tracers. The correspondence between the 18 sectors of analysis and the 3 main coronary arteries has been defined. The reproducibility of the results is excellent. The multiparametric approach of this program should be particularly useful to quantify the extent and severity of the large myocardial defects but should also help to characterize faint abnormalities.

## ACKNOWLEDGMENTS

Thanks are due to Sophra Medical Vision International and General Electric Medical Systems (Buc, France) for their support.

## REFERENCES

1. Van Train KF, Areeda J, Garcia EV, et al. Quantitative same-day rest-stress technetium-99m-sestamibi SPECT: definition and validation of stress normal limits and criteria for abnormality. *J Nucl Med.* 1993;34:1494–1502.
2. Van Train KF, Garcia EV, Maddahi J, et al. Multicenter trial validation for quantitative analysis of same-day rest-stress technetium-99m-sestamibi myocardial tomograms. *J Nucl Med.* 1994;35:609–618.
3. Germano G, Kavanagh PB, Waechter P, et al. A new algorithm for the quantitation of myocardial perfusion SPECT. I. technical principles and reproducibility. *J Nucl Med.* 2000;41:712–719.
4. Sharir T, Germano G, Waechter PB, et al. A new algorithm for the quantitation of myocardial perfusion SPECT. II. validation and diagnostic yield. *J Nucl Med.* 2000;41:720–727.
5. Slomka PJ, Hurwitz GA, Stephenson J, Craddock T. Automated alignment and sizing of myocardial stress and rest scans to three-dimensional normal templates using an image registration algorithm. *J Nucl Med.* 1995;36:1115–1122.
6. Slomka PJ, Hurwitz GA, St Clement G, Stephenson J. Three-dimensional demarcation of perfusion zones corresponding to specific coronary arteries: appli-

cation for automated interpretation of myocardial SPECT. *J Nucl Med.* 1995;36:2120–2126.

7. Benoit T, Vivegnis D, Foulon J, Rigo P. Quantitative evaluation of myocardial single-photon emission tomographic imaging: application to the measurement of perfusion defect size and severity. *Eur J Nucl Med.* 1996;23:1603–1612.
8. He ZX, Maublant JC, Cauvin JC, Veyre A. Reorientation of the left ventricular long-axis on myocardial transaxial tomograms by a linear fitting method. *J Nucl Med.* 1991;32:1794–1800.
9. Cauvin JC, Boire JY, Maublant JC, Bonny JM, Zanca M, Veyre A. Automatic detection of the left ventricular myocardium long axis and center in thallium-201 single photon emission computed tomography. *Eur J Nucl Med.* 1992;19:1032–1037.
10. Scellier D, Aktouf Z, Boire JY, Bertrand G, Maublant J. Skeletonization method for automated myocardial SPECT quantification. In: Arcelli C, Cordella LP, Sanniti Di Baja G, eds. *Advances in Visual Form Analysis.* Singapore: World Scientific Publishing; 1997:462–471.
11. Serra J. *Image Analysis and Mathematical Morphology.* New York, NY: Academic Press; 1982.
12. Blum H. A transformation for extracting new descriptors of shape. In: Wathen-Dunn W, ed. *Models for the Perception of Speech and Visual Form.* Cambridge, MA: MIT Press; 1967:362–380.
13. Calabi L, Hartnett WE. Shape recognition, prairie fires, convex deficiencies and skeletons. *Am Math Mon.* 1968;75:335–342.
14. Bertrand G, Malandain G. A new topological segmentation of discrete surfaces. Proceedings of the 2nd European Conference on Computer Vision (ECCV'92). Santa Margherita, Ligure, Italy; 1992:710–714.
15. Cauvin JC, Boire JY, Maublant J. Automatic quantification of myocardial defects by morphological methods in SPECT. *IEEE 12th Annual International Conference of Engineering in Medicine and Biology.* Philadelphia, PA; 1990:415–416.
16. Scellier D, Boire JY, Wieczorek F, et al. Improvement of automatic quantification of  $^{201}\text{Tl}$  and  $^{99\text{m}}\text{Tc}$ -sestamibi SPECT images by fuzzy segmentation [abstract]. *J Nucl Cardiol.* 1995;2(suppl):S37.
17. Faouros P, Fillard JP, Artus A. A new approach to fuzzy partition for image segmentation. *IEEE 14th Annual Conference of Engineering in Medicine and Biology.* Paris, France; 1992:1922–1923.
18. Scellier D, Boire JY, Maublant J, Veyre A. Fuzzy logic for the segmentation of myocardial tomoscintigraphic images. *IEEE 18th Annual Conference of Engineering in Medicine and Biology.* Amsterdam, The Netherlands; 1996:1500–1503.
19. Bland JM, Altman DG. Statistical methods for assessing agreement between two methods of clinical measurement. *Lancet.* 1986;1:307–310.
20. Scellier D, Boire JY, Thouly C, Maublant J. Application of skeletonization algorithms for myocardial SPECT quantification. *Lecture Notes Comput Sci.* 1996;1176:227–236.
21. Wolfe CL, James DF, Corbett JR. Determination of left ventricular mass using single-photon emission computed tomography. *Am J Cardiol.* 1985;56:761–764.
22. Nuyts J, Suetens P, Oosterlinck A, De Roo M, Mortelmans L. Delineation of ECT images using global constraints and dynamic programming. *IEEE Trans Med Imaging.* 1991;10:489–498.
23. Mortelmans L, Nuyts J, Van Pamel G. A new thresholding method for volume determination by SPECT. *Eur J Nucl Med.* 1986;12:284–290.
24. Zadeh LA. Fuzzy sets. *Information Control.* 1965;8:338–353.
25. Verberne HJ, Habraken JB, Van Royen EA, et al. Quantitative analysis of Tc-99m-sestamibi myocardial perfusion SPECT using a three-dimensional reference heart: a comparison with experienced observers. *Nucl Med Commun.* 2001;22:155–163.
26. Maddahi J, Van Train K, Prigent F, et al. Quantitative single photon emission computed thallium-201 tomography for detection and localization of coronary artery disease: optimization and prospective validation of a new technique. *J Am Coll Cardiol.* 1989;14:1689–1699.
27. Kiat H, Van Train KF, Friedman JD, et al. Quantitative stress-redistribution thallium-201 SPECT using prone imaging: methodologic development and validation. *J Nucl Med.* 1992;33:1509–1515.
28. Deychak YA, Segal J, Reiner JS, et al. Doppler guide wire flow-velocity indexes measured distal to coronary stenosis associated with reversible thallium perfusion defects. *Am Heart J.* 1995;129:219–227.
29. Kern MJ, Donohue TJ, Aguirre FV, et al. Clinical outcome of deferring angioplasty in patients with normal translesional pressure-flow velocity measurements. *J Am Coll Cardiol.* 1995;25:178–187.
30. Thouly C, Cachin F, Boire JY, Lipiecki J, Maublant J. Automatic assessment of the kinetic myocardial function in gated-SPECT [in French]. *Med Nucl.* 2001; 25:699–708.